Journal of Applied Sciences

ISSN 1812-5654

Journal of Applied Sciences 11 (5): 752-767, 2011
ISSN 1812-5654 / DOI: 10.3923/jas.2011.752.767

Geochemistry and Geotectonic Setting of Neoproterozoic Granitoids from Artoli Area, Berber Province, Northern Sudan

[1]N.H. Lissan and [2]A.K. Bakheit
[1]Faculty of Earth Resources, China University of Geosciences, Lumo Road, Wuhan, China
[2]Department of Geology and Mining, College of Natural Resources, University of Juba, Khartoum, Sudan

Abstract: The research aimed at deciphering the genetic relationship of the Artoli area, Berber Province, Northern Sudan with the domains of Saharan Metacraton and Arabian Nubian Shield and tries to define the boundary between them. In order to determine the tectonic environment, the petrographic characteristics and the original protoliths of granitoid rocks occurring within the area, several discrimination and variation diagrams were constructed using their whole-rock geochemical analysis and integrated with field observations and petrographic investigations. The results revealed that the rocks constitute voluminous, intermediate to acidic granitoidal batholith of granodiorite, quartz-diorite and diorite with lesser amount of granite that emplaced in a crystalline Proterozoic basement complex, comprising of low-grade schistosed metavolcanic rocks and minor high-grade metasediments. The Artoli granitoids are identified as medium-to high-K, calc-alkaline, metaluminous and I-type granitoid suite emplaced as volcanic arc granites above a Noeproterozoic subduction zone during the syn- to late-collision stages of crust evolution. The magmas of these granitoids were derived from the mantle with involvement of minor crust components. The overall geological and geochemical characteristics of the Artoli granitoids are comparable to the plutonic rocks of the Arabian-Nubian shield in Arabia, Egypt and NE Sudan. Thus, the area considered as a part of the westernmost Nubian Shield with its boundary with Saharan Metacraton lying further west.

Key words: Artoli granitoids, geochemistry N Sudan, Nubian tectonics, I-type granite Sudan, Berber plutonics, Nubian Shield Sudan

INTRODUCTION

The Artoli area, which constitutes the study area for this research, is an area of about 1250 km^2 lying some 56 km northeast of Atbara city, Berber Province, in northern Sudan, between latitudes 18°11′ and 18° 20′ N and longitudes 33° 55′ and 34° 05′ E (Fig. 1A, B) .

With the exclusion of some sporadic outcrops of Mesozoic sandstones (Nubian Sandstone Formation), rare and localized Paleozoic sediments (the Maki Series) and scattered Tertiary volcanics, most of the region of N and NE Sudan is exposed crystalline metamorphic rocks belonging to the Precambrian Basement Complex. This basement constitutes two major lithological associations, representing two fundamentally different crustal entities; commonly referred to as the Saharan Metacraton (SMC) in the west and the Arabian Nubian Shield (ANS) to the east (Vail, 1985; Abdelsalam *et al*., 1995; Stern *et al*., 1994). The Artoli area is situated at the inferred transition between this reworked older crust of the SMC and the Neoproterozoic juvenile; mainly green schist facies, accreted arc terranes of the ANS.

The SMC represents a Palaeoproterozoic, continental crust, dominated by heterogeneous high-grade (amphibolite facies) gneisses, migmatites and supracrustal rocks of ensialic geochemical affinities that remobilized during the Neoproterozoic time (Kroner *et al*., 1987; Kuster and Liegeois, 2001; Abdelsalam *et al*., 2002).

The ANS is a Neoproterozoic orogenic collisional belt of juvenile crust that extends from southern Israel through western Arabia, eastern Egypt and northeastern Sudan into Eritrea and Ethiopia. The shield believed to be intra-oceanic island arc/back arc-basin complexes that formed as a consequence of the convergence of East and West Gondwana and the closure of the Mozambique ocean around 870 50 Ma (Kroner *et al*., 1987; Stern, 1994). The resultant crust accreted against the SMC by the end of the Proterozoic and experienced Pan African deformation, metamorphism and plutonism events around 520 Ma (Vail, 1985; Stern, 1994; Grenne *et al*., 2003). The shield consists of a series of volcano-sedimentary terranes of low to medium metamorphic grade rocks. Situated within these terranes, are a number of NE-SW to N-S trending, ophiolite-remnants decorated belts (Fig. 1A)

Corresponding Author: N.H. Lissan, International Cooperation Office, China University of Geosciences, Lumo Road, Postcode 430074, Wuhan, Hubei, China Tel: 00868986127225 / 086275923529

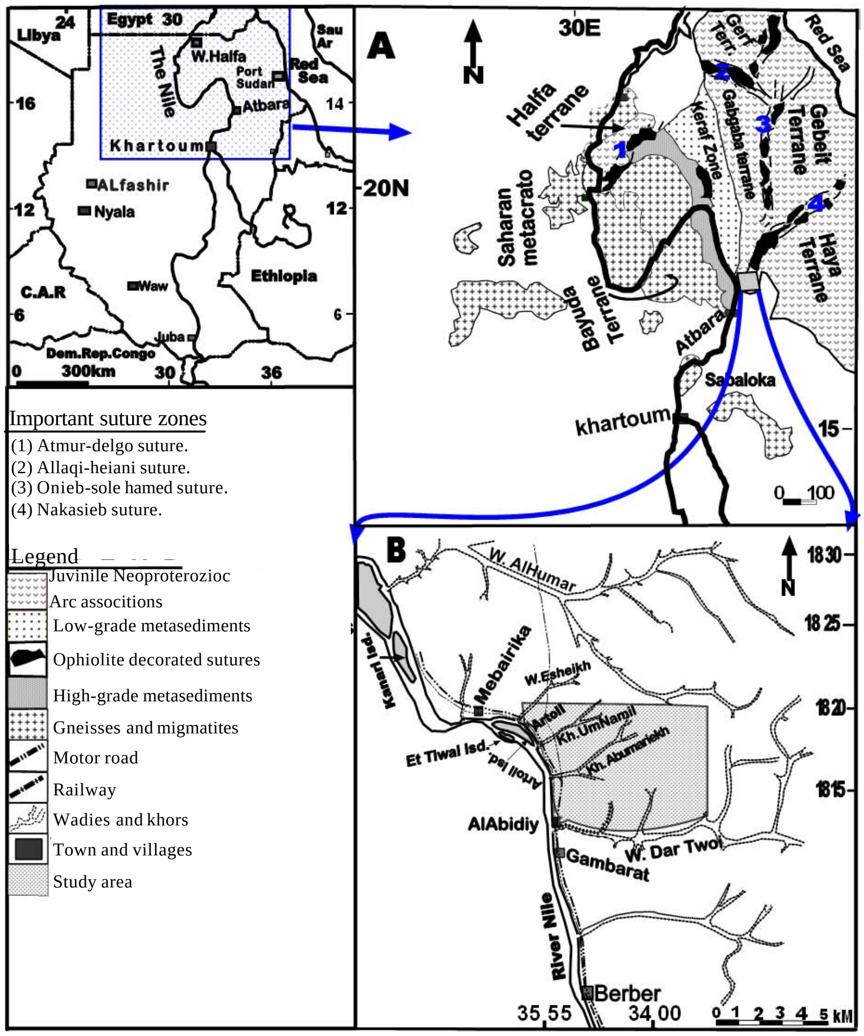

Fig. 1: Locality map for; (A) A part of NE Sudan showing major terranes and important suture zones, modified after Kuster and Liegeois (2001), (B) Artoli area

and intercalations of locally isolated moderate-to-high-grade gneiss terranes, all of which are invaded by voluminous plutonic suites. It was subsequently buried by Phanerozoic sediments but has been exposed by uplift and erosion on the flanks of the Red Sea in Oligocene and younger times (Stern, 1994; Dalziel, 1997).

The present idea on the geotectonic crustal evolution of the ANS is that the shield developed through four main stages (Gass, 1981; Stern and Kroner, 1993). During the first stage (950-850 Ma) rifting followed by sea-floor spreading and the initiation of subduction resulted in formation of oceanic crust and island arcs terranes. The second stages (850-650 Ma) dominated by welding and accretion of oceanic and island arc terrains to form the shield. The third stage (650-580 Ma) is the post-collision batholithic stage, characterized by large-scale calc-alkaline magmatism, mainly of intermediate to felsic composition. The fourth stage (600-530 Ma) is the so called the post-orogenic stage; representing intracratonic within-plate magmatism characterized by igneous activity of mainly alkaline to peralkaline granites andesites, rhyolites and several episodes of dike swarms.

The eastern boundary of the SMC in N and NE Sudan is defined by the N-S trending, ophiolite-decorated, 500 km-long and 30-150 km wide structural belt known as the Keraf- Suture Zone (KSZ) (Fig. 1A). This suture has been interpreted as an arc-continental, tectono-lithological suture that resulted from NW-SE oblique collision between the SMC and the ANS (Abdelsalam *et al*., 1995). The KSZ has rock assemblage comprising; high to medium- grade gneisses, siliciclastics, carbonate-rich low-grade metasediments, ophiolitic nappes, molasse-type sediments and post-tectonic granitoids (Abdelsalam *et al*., 2002).

The Late Proterozoic to Early Paleozoic times were characterized by a widespread igneous activity occurred in response to convergence along the margins of Gondwana. Consequently, abundant voluminous plutonic rocks of different ages and tectonic evolution intruded the N and NE Sudan's Precambrian crystalline basement terrains. These are mainly; (1) Syn-to late -orogenic granitoid assemblages (880-610 Ma). (2) Post- to an-orogenic granitoid assemblages (600-475Ma) previously known as the older and younger granitoids, respectively (Neary *et al*., 1976; Almond, 1982; Noweir *et al*., 1990).

Numerous studies have been conducted concerning the petrogenetic and geotectonic evolution of the basement rocks from the SMC, ANS and KSZ. However, controversy persists on the mode and nature of tectonic and geological evolution of these rocks and their associated ore deposits in some areas of the region, in addition to the location and nature of the boundary between the ANS and SMC (Almond, 1982; Abdelsalam *et al*., 1995). Understanding the origin and geotectonic setting of the granitoid rocks will contribute to the resolution of this controversy.

In this study, we have combined the results of field, petrographical and geochemical investigations on the intrusive rocks from Artoli area in order to provide constraints on the petrographic characteristics, original protoliths and the geotectonic setting of these rocks. It is also meant to determine the relation of the area with the Arabian-Nubian Shield, Keraf-Suture zone and Saharan Metacraton by getting more information concerning the geodynamical evolution along the north-central part of the ANS/SMC boundary.

THE GEOLOGY OF THE STUDY AREA

The Artoli area constitutes a crystalline basement terrane, with basement rock successions exposed in most parts of the area except the western most (Fig. 2). It consists mainly of a series of spatially overlapping metamorphosed complex, the dominant rocks of which are low-grade schistosed metavolcanics with subordinate high-grade metasedimentary rocks. Both are intruded by various generations of syn- to late-orogenic granitoids and post-orogenic minor intrusions and covered locally in some parts, by Nubian Sands and Recent superficial deposits (Lissan and Bakiet, 2010). The contact relations among the basement rocks extensively modified by superimposed metamorphic and deformation events, hence, integration of obvious lithological difference, metamorphic extents, field appearance and structural styles were used to classify the rock succession of the area into the following units (Fig. 2).

High-grade metasedimentary rocks: This group constitutes the oldest rocks (Plaeproterozioc) in the map area and is mainly concentrated in the western and northwestern parts as a local inlier in a narrow belt extending in N-S direction (Fig. 2). The sedimentary origin of these high-grade rocks is inferred in the field from the heterogeneous nature, frequent intercalation feature and the short-distance facie change. There is no sufficient field evidences for precise contact relations between this suite ant the other groups, as the underlying group is not exposed and the contacts with the overlying rocks are extensively modified by superimposed deformation and metamorphic events and obliterated by screes and alluvial deposits. However, the suite everywhere studied in the region ascertained to be disconformably overlying high-grade gneisses and structurally overlain by Low-grade volcano sedimentary series (Almond, 1982). The suite comprises variably interbedded lithologies of biotite-gneiss, quartzo-feldspathic gneiss, quartzite, marbles and amphibolites.

The biotite-gneisses, in general, are leucocratic to mesocratic, medium-grained rocks exhibiting moderate gneissic layering in a NW-SE direction coinciding with the regional trend defined by parallel alignment of biotite and hornblende alternating with elongated quartz and plagioclase grains. Under the microscope the gneiss shows a simple mineral assemblage composing of angular to subangular quartz crystals within predominate orthoclase feldspars and minor plagioclase (albite-oligoclase composition); both may be altered to turbid sericite. Of the mafic minerals, oriented yellow biotite flakes by far exceed green hornblende, muscovite and garnet. Fe-oxides are unmissed with zircon, apatite and opaques as accessories.

The quartzo-feldspathic gneiss is exposed along dry streams with the above unit at the central-west part as rather all-weathered surfaces concealed under variable thickness of alluvial sands and lag deposits. It is medium to coarse-grained, light to grayish and with detectible gneissic banding in a NW trend. Pterographically, consists of quartz, feldspars, yellowish brown biotite, few flakes of muscovite and prisms of hornblende. Secondary minerals of epidote, sericite and chlorite are commonly developed after mafic minerals. Accessories of apatite, zircon, sphene and iron oxides are also conspicuous.

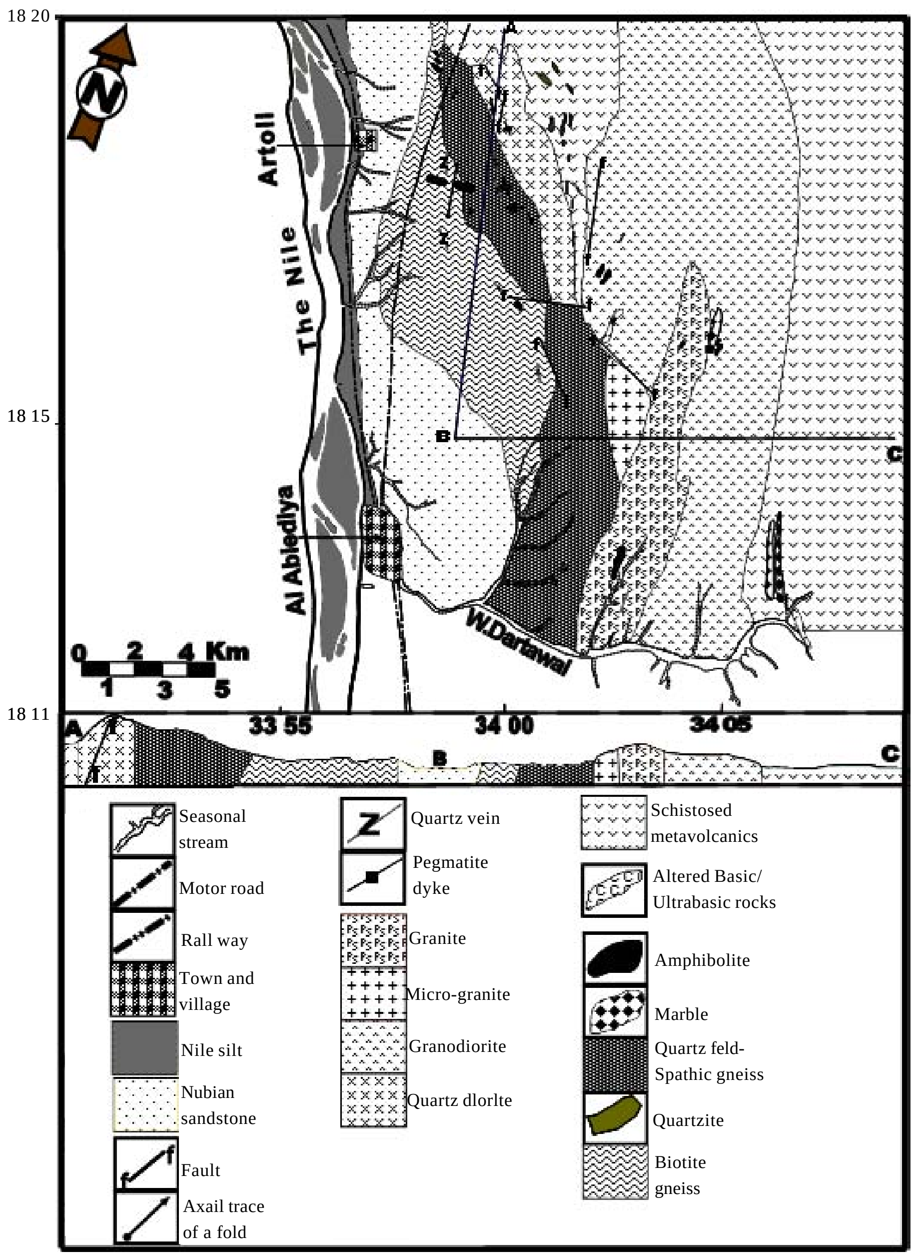

Fig. 2: Geological map of the study area

Quartzitic rocks are encountered in the eastern and the central parts of the map area as relatively outstanding ridges extending in a NE direction for considerable distance probably tracing a linear regional pattern representing fault zone (Fig. 2). The quartzites are compact, brecciated rocks or may be banded (Umtrambeish area), varying from white to ferruginous reddish brown or grey varieties. In thin section, they show abundant stout granular quartz crystals besides, few silvery muscovite flakes, plagioclase and K-feldspars.

Marbles occur in most parts of the area especially in the eastern part as irregular bands, thin layers and lenticular or tabular-shaped bodies, seldom exceed a few meters w ide (0.5-8 m). Most marbles are medium to coarse-grained, massive rocks ranging from pure sugary white to impure shaded grayish, dark gray, yellowish brown or buff coloured. The pure varieties show granoblastic texture, the sheared ones may show distinct cataclastic textures. 70-80% of the rock composition is interlocking crystalline calcite with clear twin lamellae and the remaining is mostly equigranular, fine-grain quartz, sericite and plagioclase. Some mica and epidote are accessories.

Mafic amphibolites are conformably intercalated with the gneisses in the NW part, as sporadic lens-shaped or patches only few meters thick. They are generally recognized by their dark to dark gray colour and medium-grained texture and commonly show megascopic preferred mineral segregation banding in accord with regional trend emphasized by preferred orientation of hornblende prisms and aligned felsic minerals. The amphibolites are fine to medium-grained rocks disclosing a mineral association comprising; hornblende, plagioclase and quartz as essentials, chlorite, epidote, sericite and biotite as secondary and sphene, apatite, zircon, iron oxides, garnet and pyrite as accessories ones.

Low-grade schistosed metavolcanics rocks: In the study area, low-grade, green schist facies rocks that are predominant metavolcanics associated with minor sedimentary units encountered exposed in the neighborhood of Umtrambeish ore field, in addition to small sporadic outcrops in the granitoids plain to the north (Fig. 2). This group of rocks usually has a gradational boundary with the underlying units and includes metamorphosed basic to intermediate-acidic volcanic rocks that show varying degrees of deformation, ranging from massive, undeformed bodies to strongly schistosed rocks. Most of them are fine-grained with primary volcanic textures still recognizable (porphyritic and sometimes amygdaloid). Under the microscope, most rocks contain quartz, sericitized plagioclase, chlorite and actinolite, besides K-feldspar, opaques, calcite and some rare relict pyroxene. This mineral assemblage and the shown textures are indicative features of green-schist facies metamorphism of originally volcanic rocks. Based on field and petrographic data, theses schistosed rocks are classified into; quartz-mica schist, sericite-chlorite schist and actinolite-schist.

The quartz-mica schists characterized by clear microfolds, crenulation cleavages, nearly vertical dips and well defined schistosity. They are gray to light-greenish gray coloured rocks of fine texture and often disclose a typical low-grade mineral assemblage comprising; quartz, chlorite, muscovite, minor biotite and subordinate sericite, plagioclase, epidote and calcite with common accessories of sphene, apatite, iron-oxides and garnet.

The sericite-chlorite schist is greenish to greenish-gray coloured rock of fine-grain texture and exhibit profound schistosity. Minerogically, it shows lepidoblastic to garnoblastic appearance in sericite, chlorite, plagioclase, quartz and minor biotite, besides epidote, iron oxides and calcite with accessory minerals of apatite and pyrite.

The actinolite-schists are fine-gained green-coloured rocks found predominantly around Umtrambeish area. Under the microscope, they show almost a complete alteration testified by the high abundance of green minerals. The mineral assemblage is a combination of irregularly oriented bright green actinolite, elongated and highly altered plagioclase, dragged crystals of quartz, aggregated epidote, turbid and anhederal crystals of calcite, small, spindle-shaped granules of sphene and rounded apatite.

Syn-to late-orogenic granitoid rocks: Vast masses of intermediate to acidic granitoids constitute a characteristic and dominant element of the basement rocks of the area. This granitoid suite is believed to be a product of larger plutons of syn, to late-orogenic igneous activities in the late Proterozioc time that have been emplaced in both the high and low-grade sequences as evident from their xenolithic contents. Based on field and petrographic evidences, they are generally range in composition from diorite, quartz diorite, to granites, but predominantly are hornblende granodiorites (Fig. 2).

The diorite occurs together with the granodiorite as large, round-shaped bodies in the northern and central sectors, where they form about 50% of the outcrops. It is fine-to medium-grained rock with nearly equal proportions of mafic and felsic constituents. The dominant mafic mineral is actinolitic hornblende, which is partly to completely altered to aggregates of chlorite, calcite and epidote. The plagioclase feldspar occurs as subhedral aligned laths, which form strongly zoned crystals. The most common accessory minerals are magnetite, titanite and apatite.

Quartz dioritic rocks occur as excellent exposures of low to moderate relief in the NW part of the mapped area. Macroscopically, they are gray coloured rocks usually devoid of pervasive foliation, but the intense deformation caused some verities to develop a slight banding. Petrographically, they are coarse hypidiomorphic rocks in which felsic minerals constituent more than 60%, of which quartz form about 10%, the other minerals are slightly sericitized plagioclase, coarse subhedral hornblende, as main primaries, oriented pale-brown pleochoric biotite, mostly untwined orthoclase and perthites as minor phase and sphene, zircon, titanite, apatite, pyrite and magnetite as accessories. Secondary minerals are sericite, chlorite, epidote and carbonates.

Granodiorites constitute a wide range of rocks found in association with minor granites in the central part of area (Fig. 2). The rocks are relatively homogenous, medium to coarse-grained, gray to grayish dark in colour and mostly altered and deformed types to the extent that all gradation from the moderately massive to completely foliated types exist. Microscopic observation revealed coarse hypidiomorphic granular texture and disclosed main mineral phases of subhedral to euhedral crystals of plagioclase exhibiting deferent degree of alterations (to sericite and chlorite), pleochoric prisms of hornblende, quartz grains commonly showing ragged boundries with strongly undulose extinction (form about 10%), oriented pale to dark-brown pleochoric biotite, sericite, chlorite, small columnar epidote, highly sericitized and discontinuously zoned k-feldspar, perthites, opaques, actionlite and kaolin. Hexagonal apatite is a frequently abundant accesstory mineral with zircon, titanite and sphene.

Granites and micro-granites constitute only minor discrete intrusion phases within the granodiorite sequence and believed to be emplacement products of the last intrusion phase to which the area was subjected. These rocks are granites in the strict petrologic meanging of the term. They are coarse to medium-grained, light to gray rocks; most of them are intensely deformed and sheared to the extent of foliation and partial destruction of the granitic features. Under the microscope, they show a granitic texture formed by pink K-feldspar phenocrysts in affine cloudy quartz and feldspar matrix associated with lesser amount of mafic minerals; sub-hedral flakey, brown biotite, green hornblende, chlorite, epidote and sericite and accessories of zircon, apatite and iron oxides.

Post-orogenic minor intrusions: Commonly numerous quartz veins and lesser amounts of pegmatitic bodies together with scarce acidic and basic dykes are observed invading the country rocks throughout the area. Occurrence of these bodies with the associated alteration features suggests an intense hydrothermal activity. They are strongly deformed, broadly discordant and irregular or lensiod bodies maintaining a common sinuous feature expressed mainly through swinging along N-S and NE-SW directions with steep dip westwards. In the field, the pegmatites seem to be older than most generations of quartz veins as the later found terminating against the former.

The pegmatites are very coarse-grained massive rocks made up essentially of aggregates of coarse crystals of alkali-feldspar (orthoclase and microcline), quartz, some plagioclase, few mica flakes tourmaline and apatite.

A number of scattered acidic and basic dykes are found cutting the different units of the basement complex. The dykes are generally short narrow bodies (0.5-1.0 m in width and rarely traceable for more than 3 m) occurring in contrast colour with host rocks. Lithologically, typical granitic dykes (aplitic and granophyric) predominate, though dark and fine-grained basic dikes are also present. The acidic dykes are fine-grained, white to pale pinkish rocks and show equigranular textures. They contain quartz, K-feldspar, variably altered plagioclase and biotite flakes.

The quartz veins represent an important episode in the history of the area since their emplacement was connected with the hydrothermal activities that brought about the gold mineralization. They are of variable sizes ranging from stringers, pods and narrow veins up to wide ones. A close examination reveals that more than a generation exists in the area; (1) the first one comprises early and widespread veins that are mainly concordant, deformed and folded with enclosing rocks (more than 200 m in length, few cm to 3 m width). The veins of this type exhibit varying colours, white, grey, milky, smoky, yellowish, brown, reddish or stained greenish depending on weather the quartz is pure, contaminated or stained by iron oxides or malachite. This type seems to be introduced along major structures and older shear zones. The veins are characterized by pinching and swell feature laterally and vertically and are associated with the main gold mineralization in Umtrambiesh area. (2) The second generation represents a younger phase of less abundant veins with more wider dimensions compared with the first generation, found striking in NW-SE or E-W direction and occur as discontinuous, crashed and patchy bodies. This type of veins is often barren clean whitish quartz with some tourmaline crystals. Some smoky, gray and pink types are present.

ANALYTICAL METHODS

Several representative samples encompassing the compositional and spatial ranges of plutonic rocks (not including micro-granite) were collected from the Artoli area, northern Sudan, through surface mapping that executed during tow field trips collectively lasted for seven weeks on November and January of 2005. Twenty-seven samples were petrographically selected for whole-rock chemical analyses. The samples were submitted through Rida Mining Company, Sudan to the ACME Analytical Laboratories, Vancouver, Canada for analytical work and calibration against international standards. The analytical results are listed in Table 1-3.

Whole rock element compositions were determined using inductively coupled plasma-atomic emission spectroscopy (ICP-ES) technique at ACME Analytical Laboratories, after lithium metaborate /tetraborate fusion and dilute nitric acid digestion of rock powder. Replicate analyses for some major and trace elements for some key samples were carried out by X-ray fluorescence spectrometry technique (XRF) following standard techniques and using a Phillips Venus 200 XRF instrument at the analytical laboratories of the Geological Research Authority of the Sudan (GRAS).

All major element values cited in Table 1 and used in plots, were recalculated to 100% on an anhydrous basis. Loss on Ignition (LOI) was determined from total weight loss after repeated ignition of the powdered samples at 1000°C for 1 h and cooling. Satisfying analytical accuracy was achieved by using replicate analyses and compared with rock standards.

RESULTS

Twenty seven whole-rock samples of plutonic rocks from the area have been analyzed for major/minor element oxides and selected trace and rare earth elements (Table 1-3) and their chemical data are used in the following interpretation.

Chemical alteration and element mobility: Although, alteration of plutonic rocks is a common phenomenon, in particular for Proterozoic rocks, most of the analyzed samples showed only slight or no substantial mobility during late-phase alterations of the plutonic rocks. This is inferred from the linear trend in Harker (1909) variation diagrams (Fig. 3), the medium-to high content of Ca_2O and K_2O, the 33±10 alteration index (Ishikawa *et al*., 1976):

$$(A.I. = [(MgO+K_2O) /(MgO+K_2O+CaO+Na_2O)]*100$$

and the reliable loss on ignition (LOI) values (Table 1, 4). Thus, the element signatures may reflect the composition of their protolith.

Rock classification: On the total alkali-silica TAS, {SiO_2 vs. ($Na_2O + K_2O$)} geochemical rock classification diagram (Wilson, 1989) used for classification of the granitoid rocks of the area, the samples are plotted in the diorite, quartz-granodiorite and granite fields (Fig. 4a) in an agreement with the petrographic characteristics of the rocks. A sample of the rocks defined from the field and petrographic data as quartz-diorite and granodiorite are classified chemically as granite and another sample from the granites plot as quartz-diorite, a phenomenon may be attributed to the mobility of Na and K during hydrothermal alteration. The normative Ab-An-Or diagram of Barker (1979), also confirms the facts of predominance of granodioritic to quartz-dioritic compositions among the Artoli granitoids and the designation of few samples from them as granites (Fig. 4b). On both diagrams, a few them as granites (Fig. 4b). On both diagrams, a few samples straddle the boundary between the quartz-granodiorite and granite fields.

Major element characteristics: The Artoli plutonic rocks display a marked variation in the abundance of some major elements, mostly in ranges of SiO_2, Fe_2O_3, CaO, TiO_2

Table 1: Major elements data of plutonic rocks from Artoli area

Sample	SiO_2	TiO_2	Al_2O_3	Fe_2O_3	MnO	MgO	CaO	Na_2O	K_2O	P_2O_5	LOI	Total
QzD1	69.75	0.36	12.50	3.05	0.06	1.90	2.68	5.32	3.09	0.11	0.50	99.32
QzD2	64.00	0.71	12.00	6.13	0.12	3.14	4.66	4.21	2.97	0.16	0.80	99.89
QzD3	66.15	0.61	14.06	4.27	0.20	1.52	7.11	3.70	2.15	0.10	0.40	100.27
QzD4	66.20	0.91	14.00	4.75	0.08	1.76	6.13	3.60	2.12	0.17	0.50	100.22
QzD5	68.15	0.64	14.04	4.26	0.08	1.68	4.82	3.99	2.83	0.08	0.40	100.97
QzD6	65.37	0.87	14.00	5.35	0.10	1.92	5.43	4.05	2.90	0.23	0.30	100.52
GD1	65.17	0.60	14.15	3.77	1.11	1.80	4.51	4.61	3.74	0.16	0.40	100.02
GD2	67.55	0.34	13.28	3.58	0.11	1.62	5.34	4.86	2.68	0.13	0.50	99.99
GD3	68.21	0.34	11.63	4.48	0.19	1.99	4.86	4.74	1.99	0.05	1.50	99.98
GD4	65.14	1.21	9.27	5.92	1.12	2.99	8.35	4.09	1.76	0.15	0.30	100.30
GD5	63.15	0.92	13.13	5.15	0.16	3.80	5.15	4.46	3.36	0.36	0.60	100.24
GD6	63.40	0.64	14.18	5.81	0.53	2.34	6.65	4.89	1.77	0.15	0.40	100.76
GD7	62.97	0.55	9.45	6.71	0.22	2.81	10.00	3.68	3.13	0.06	0.50	100.08
GD8	66.79	0.67	8.78	7.02	0.26	2.68	7.51	3.79	1.92	0.06	0.60	100.08
G1	71.17	0.13	13.40	1.23	0.04	0.35	5.24	4.93	3.92	0.03	0.10	100.54
G2	72.06	0.35	12.45	1.54	0.05	0.17	6.27	4.43	2.14	0.13	0.60	100.19
G3	70.13	0.30	14.05	3.16	0.06	0.42	2.98	4.71	4.53	0.17	0.50	101.01
G4	68.24	0.46	13.25	3.14	0.05	1.93	3.32	4.86	4.63	0.11	0.17	100.16
G5	67.42	0.20	15.00	5.02	0.14	0.23	2.28	5.17	3.93	0.04	0.40	99.83
G6	65.00	0.67	13.15	4.24	0.12	3.70	5.13	5.17	2.50	0.35	0.30	100.33
G7	68.17	0.40	12.12	3.95	0.05	2.10	5.45	4.18	3.12	0.13	0.40	100.07
G8	71.17	0.38	13.12	2.36	0.13	1.38	4.18	4.11	2.74	0.11	0.50	100.18
D1	57.15	1.63	13.18	7.17	0.14	6.52	8.05	3.77	1.24	0.34	0.80	99.99
D2	59.24	0.62	15.69	7.13	0.09	3.35	6.76	3.93	3.13	0.13	0.50	100.57
D3	56.44	0.81	12.30	7.7	0.21	5.75	11.06	3.40	1.82	0.22	0.70	100.41
D4	57.66	1.15	13.29	7.94	0.13	6.16	7.80	3.46	1.66	0.33	0.50	100.08
D5	57.19	1.22	14.11	7.37	0.10	6.53	6.53	3.63	2.91	0.25	0.70	100.54

Table 2: Selected trace elements abundances of plutonic rocks from Artoli area

Sample	Ni	Sc	Nb	Sr	Zr	Y	Ba	Ga	Rb	Hf	Cr	Th
QzD1	10.0	5.00	9.90	513	154	34.0	241	11.0	51.0	5.3	185	12.40
QzD2	48.0	17.00	8.40	217	89	21.0	480	10.0	43.0	8.3	345	14.20
QzD3	0.0	241.00	9.20	270	115	23.0	241	18.0	25.0	7.1	435	16.40
QzD4	0.1	148.00	9.30	257	125	26.0	148	14.0	40.0	5.6	294	7.90
QzD5	0.1	257.00	9.80	303	155	30.5	551	16.0	28.0	5.8	412	12.70
QzD6	0.0	163.00	9.50	245	105	28.0	163	18.0	37.0	5.6	418	10.60
GD1	21.0	6.00	9.60	205	138	22.0	799	16.5	37.4	5.3	-	11.40
GD2	10.0	13.00	9.60	352	163	16.0	104	15.5	36.0	4.7	88	12.40
GD3	10.0	100.00	9.00	120	172	42.0	130	15.0	32.0	5.1	-	10.50
GD4	0.0	172.00	8.50	119	125	21.4	172	16.0	31.0	6.8	239	11.00
GD5	0.1	156.00	7.10	365	106	14.0	228	12.0	41.0	7.2	226	10.12
GD6	43.0	399.00	8.00	300	143	20.3	399	11.0	30.0	5.9	-	6.00
GD7	91.0	25.00	5.50	175	78	15.5	180	11.0	21.0	3.8	319	11.60
GD8	10.0	21.00	5.50	194	128	15.0	378	10.0	20.0	2.9	277	12.20
G1	28.0	1.00	10.60	497	217	45.2	506	10.0	40.0	6.0	-	15.00
G2	10.0	4.00	10.80	293	224	45.6	286	13.0	43.0	8.4	137	17.00
G3	10.0	4.00	10.00	109	210	40.0	370	12.0	27.0	8.9	298	19.00
G4	43.0	9.00	9.70	427	167	30.0	419	13.0	24.0	7.3	166	10.00
G5	10.0	1.00	9.40	102	169	27.0	106	11.0	30.0	-	-	8.00
G6	35.0	21.00	9.30	551	189	24.0	295	14.0	41.0	7.9	-	5.50
G7	10.0	5.00	7.00	503	177	29.0	438	14.0	37.0	8.9	53	16.00
G8	0.0	121.00	10.40	336	217	45.0	121	15.0	28.0	9.0	417	9.70
D1	40.0	24.00	7.30	653	60	16.0	239	15.5	31.0	18.0	265	8.40
D2	10.0	18.00	7.80	515	65	20.0	100	16.0	26.0	6.6	287	10.20
D3	10.0	1.00	7.40	284	67	16.5	101	13.0	24.0	6.1	298	8.25
D4	17.0	161.00	7.40	535	76	16.0	311	12.5	23.0	-“	-	4.50
D5	48.0	26.00	7.50	901	89	18.0	103	12.0	22.0	5.6	183.4	9.10

Table 3: Selected REE data of plutonic rocks from Artoli area

Sample	La	Ce	Pr	Nd	Sm	Eu	Gd	Tb	Dy	Er	Tm	Yb	Lu
QzD1	35.50	40.0	6.10	38.40	4.30	1.30	3.75	0.50	2.22	1.80	0.18	1.12	0.18
QzD2	44.40	34.0	5.80	58.10	5.10	1.20	5.19	0.62	2.70	1.33	0.19	1.33	0.21
QzD3	23.70	47.0	7.60	40.20	6.20	1.10	3.67	0.46	2.80	1.60	0.16	1.21	0.19
QzD4	20.81	69.0	4.90	38.90	5.10	1.09	3.49	0.44	2.88	1.00	0.15	0.97	0.16
QzD5	22.00	82.0	5.20	28.50	8.50	1.00	3.23	0.43	2.97	1.23	0.19	1.23	0.22
QzD6	30.90	78.0	4.61	45.97	3.90	0.87	3.90	0.52	2.36	1.10	0.20	1.18	0.18
GD1	28.00	60.0	5.70	30.00	4.00	0.98	2.99	0.49	1.97	1.05	0.19	1.32	0.17
GD2	22.00	98.0	6.70	40.00	5.50	1.18	3.75	0.47	2.00	1.14	0.18	1.17	0.19
GD5	59.30	82.0	3.50	22.40	3.00	1.00	3.32	0.31	1.85	1.09	0.17	1.14	0.20
GD7	13.40	38.4	6.30	14.00	4.00	1.40	3.80	0.80	1.79	1.30	0.34	0.97	0.18
GD8	25.80	47.7	5.30	16.60	3.30	0.73	4.40	0.50	2.30	1.78	0.30	1.12	0.14
G2	47.00	98.0	4.20	46.10	4.00	0.95	3.60	0.51	2.25	1.02	0.17	1.36	0.24
G4	34.00	112.0	2.30	23.50	3.70	1.32	3.80	0.47	2.21	1.20	0.20	1.18	0.27
G7	22.00	97.0	2.70	23.90	3.10	1.29	3.98	0.43	2.20	1.30	0.23	1.23	0.25
G8	23.00	100.0	3.55	18.40	3.61	1.18	2.70	0.40	2.19	1.40	0.26	1.30	0.29
D2	23.00	86.0	7.68	17.80	7.10	1.30	3.17	0.51	2.17	1.12	0.30	1.60	0.23
D3	25.00	86.0	6.00	15.90	6.50	1.20	3.17	0.56	2.16	1.23	0.31	1.62	0.21
D5	29.00	60.0	6.30	14.30	5.00	0.87	2.98	0.60	2.10	1.40	0.36	1.65	0.20

and MnO (Table 1). This variation, which may suggest diverse protolith, is directly correlated with modal abundance of the main mineral phase. Most samples have low iron content (Fe_2O_3) ranging between 1.23 and 7.94 wt%, with Fe_2O_3/MgO range <3, TiO_2 values are generally <1%, therefore they are in the range accepted in calc-alkaline rocks (Irvine and Barager, 1971; Pearce and Cann, 1973). Other elements fall within the normal granitic abundancy limits (Nockolds, 1954).

The major element chemistry for the Artoli granitoids show some characteristic features such as the > 1 wt% of K_2O, the < 0.8 value of Fe_2O_3/(Fe_2O_3+MgO) ratio and the less than 1.1 aluminum saturation index (Table 1, 4):

$$ASI = \text{molar } Al_2O_3/CaO+Na_2O+K_2O$$

these features might indicate their probable arc environment of emplacement. Furthermore, this ASI <1.1 ratio is also a distinctive chemical property of the I-type granitoids according to Chappell and White (1974).

Selected major element oxides and trace elements have been plotted against SiO_2 in Harker variation diagrams (Fig. 3) to evaluate trends associated with primary igneous processes or secondary element mobility. Most of the elements display rather regular trends of good correlation with silica (SiO_2), indicating normal igneous trends. There is a decrease in TiO_2, Fe_2O_3, MgO and CaO contents and corresponding increase in Na_2O and K_2O with increasing silica. These linear trends might indicate that the concentrations of most elements are not significantly changed from their primary abundances.

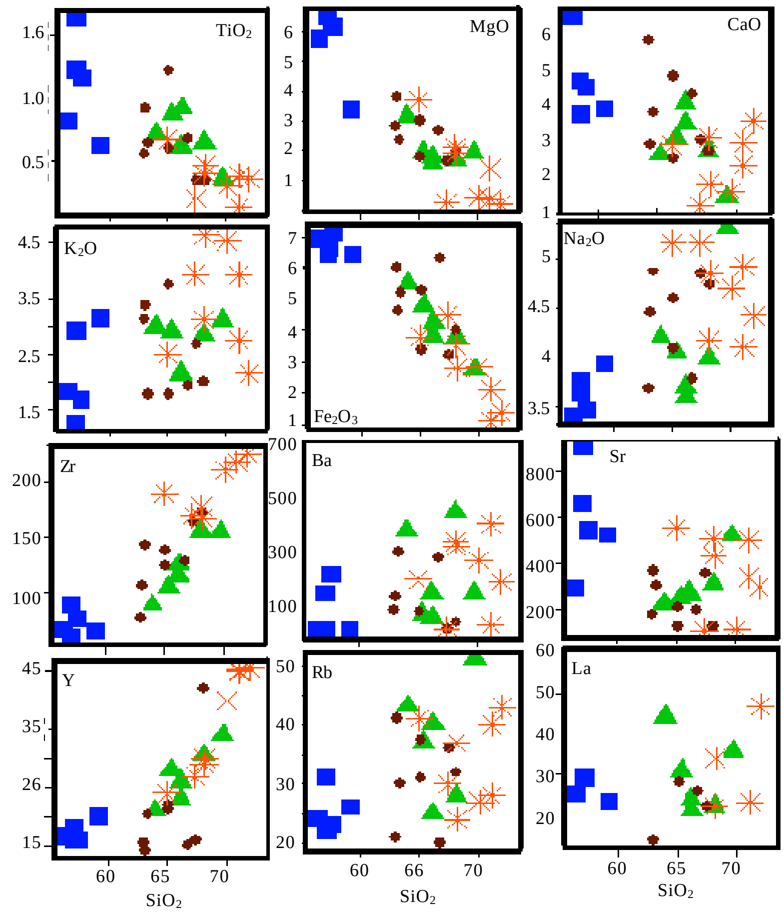

Fig. 3: Harker variation diagrams; silica (SiO_2 wt%) plotted against a range of major (in wt%) and selected trace elements (in ppm) for the Plutonic rocks of the study area. (Symbols: Closed triangle green: Quartz-diorite, closed circle deep brown: Granodiorite, closed cubic blue: Diorite and cross star red: granite)

Al_2O_3 (not shown) shows an increasing trend until 57% silica, after which Al_2O_3 decreases due to the onset of plagioclase fractionation.

Trace and rare earth elements characteristics: The Artoli granitoid rocks are enrichment in some trace and rare earth elements content particularly; K, Rb, Sr, Th, Ce and Sm compared to Nb, Hf, Zr, Rb, Y and Yb a characteristic feature of volcanic arc (possibly I-type) granites (Pearce *et al*., 1984). The trace elements also show coherent enrichment/depletion linear trends with SiO_2 (Fig. 3). Compatible elements (Cr, Ni and Sr) consistently decrease with increasing SiO_2. Incompatible high field strength elements (Y and Zr) and large ion lithophile elements (Ba and Rb) are positively correlated with SiO_2. The REE's generally increase in abundance with increasing SiO_2 from diorites, quartz diorite to granite (Table 3).

On spider diagram (Fig. 5), multi-element profiles normalized to primitive mantle (Sun and McDonough, 1989) the granitoids have patterns showing geochemical features of island-arc granites, such as the enrichment in the Large Ion Lithophile Elements (LILE) Sr, K and Ba, relative to High Field Strength Elements (HFSE) and Heavy Rare Earth Elemrnts (HREE) Nb, Zr, Ti and Y. The samples show a prominent negative Sr, Ba Nb, P and Ti anomalies compared to the LREE and Th, which are typical characteristics observed in the subduction related granitoids (Pearce *et al*., 1984; Condie, 1998).

The chondrite-normalised Rare Earth Element (REE) diagrams (Boynton, 1984) (Fig. 6) show overall moderately steep patterns characterized by a negative slope, with overall enrichment in the LREE relative to HREE with negligible to very minor negative Eu anomalies. The patterns indicate moderately fractionated LREE and poorly fractionated HREE (Fig. 6, Table 3).

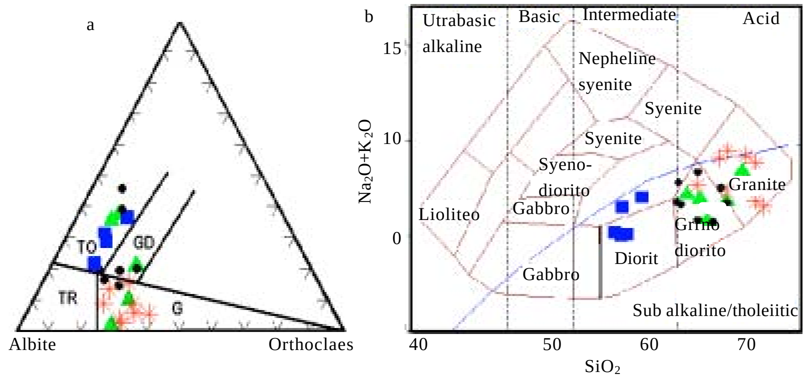

Fig. 4: (a) Normative Ab-An-Or diagram (Barker, 1979), (b) Chemical classification diagram for the Artoli plutonic rocks based on TAS, wt%, SiO_2 vs. ($Na_2O + K_2O$) of Wilson (1989). Fields: G = Granite; TR = Trondjhemite; GD = Granodiorite and; TO = Tonalite to Gabbro (Symbols: as in Fig. 3)

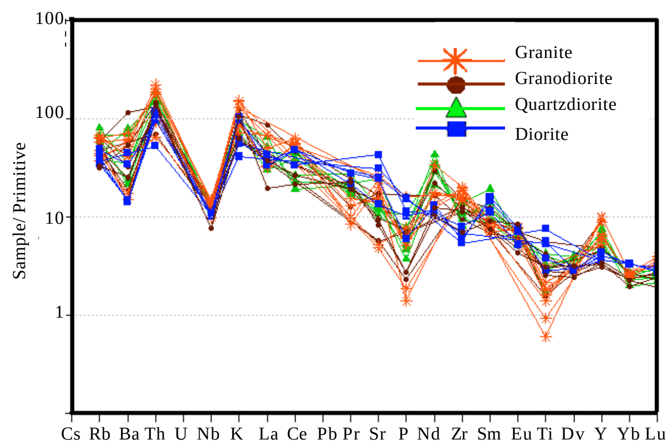

Fig. 5: Mantle-normalized multi-element diagram of the granitoid rock samples from the study area, (Sun and McDonough, 1989)

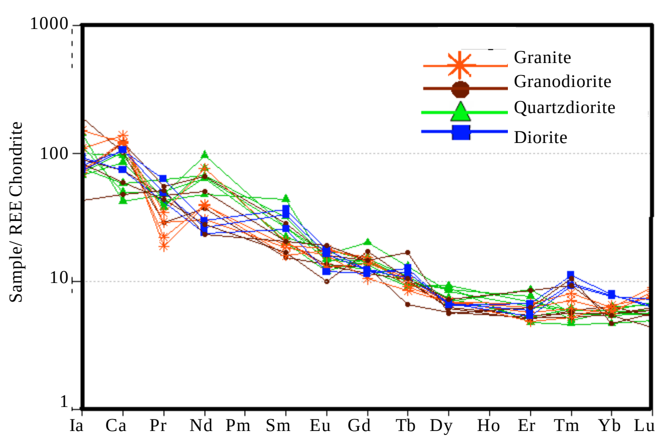

Fig. 6: Chondrite-normalized REE patterns for the Artoli granitoids, chondrite normalization values are from (Boynton, 1984)

Table 4: Some Element Ratios from the Artoli Plutonic Rocks

Sample	ASI	A.I.	F/M	F/F+M	AI
QzD1	1.090	38.4	1.61	0.62	0.67
QzD2	1.010	40.8	1.95	0.66	0.60
QzD3	1.080	25.3	2.30	0.74	0.42
QzD4	1.180	28.5	2.20	0.73	0.41
QzD5	1.080	33.9	2.54	0.72	0.49
QzD6	1.100	33.7	2.30	0.74	0.50
GD1	1.000	37.8	2.09	0.68	0.59
GD2	1.030	29.7	2.21	0.69	0.57
GD3	1.000	29.3	1.90	0.69	0.58
GD4	0.650	27.6	1.98	0.66	0.63
GD5	1.020	42.7	1.36	0.58	0.60
GD6	1.070	26.3	2.48	0.71	0.47
GD7	0.870	30.3	2.39	0.70	0.72
GD8	0.970	28.3	2.40	0.70	0.65
G1	0.950	29.6	2.51	0.78	0.66
G2	0.970	25.8	2.06	0.80	0.53
G3	1.050	39.2	2.52	0.80	0.66
G4	1.030	43.0	1.63	0.62	0.72
G5	1.040	35.8	2.26	0.86	0.61
G6	1.030	37.6	1.15	0.53	0.58
G7	0.950	35.2	1.88	0.65	0.60
G8	1.100	33.2	1.71	0.63	0.52
D1	1.020	39.6	1.10	0.52	0.38
D2	1.090	37.7	2.13	0.68	0.45
D3	0.860	34.4	1.34	0.57	0.42
D4	1.060	41.0	1.29	0.56	0.39
D5	1.080	43.2	1.13	0.53	0.46

ASI = Aluminum saturation index {=Al2O3/(CaO+Na2O+K_2O)}, A. I. = Alteration index {= (MgO + K_2O) / (MgO + K_2O + CaO + Na_2O)] *100}, F/M = Fe_2O_3/MgO, F/F+M = Fe_2O_3/(Fe_2O_3+MgO), AI = Agpaitic index {molar (Na + K)/Al}

Magma characterization: The magma type of the granitoids is illustrated by plotting the Fe_2O_3/MgO ratios against SiO_2 contents on the diagram of Miyashiro (1974) and AFM diagram of Irvine and Barager (1971), (Fig. 7), which shows that all data cluster in the calc-alkaline field indicating strong calc-alkaline affinity.

From Shand (1927) alumina saturation index diagram (Fig. 8A) appears that all units of Artoli granitoids plot exclusively in the metaluminous field. They are defined as medium- to high-K granitoids on the SiO_2-K_2O of Peccerillo and Taylor (1976) (Fig. 8B), a fact which emphasized by the less than 1.1 Alumina Saturation Indices (ASI), defined as the molecular A/CNK=Al_2O_3/(CaO+Na_2O+K_2O) (Table 4).

Granitoids of the Artoli area are exclusively of I-type nature as indicated by the alkali concentrations (K_2O-Na_2O) discrimination diagram (Fig. 9). Using the series of diagrams that employ Ga/A1 and Y, Ce, Nb and Zr against various major element ratios, designed by Whalen *et al.* (1987) to discriminate A-type granites (Fig. 10), the same result is reached, as the granitoids plot in the field of I-, S- and M-type granitoids or close to the boundary of the A-type granite

Geotectonic setting: On multicationc R1-R2 diagram of Batchelor and Bowden (1985), the tectono-magmatic character of the Artoli plutonics is specified dominantly as syn-to late-collision granitoids with minor pre- collision phase (Fig. 11). When the granitoids are plotted on a Y versus Nb diagram using the compositional discriminant fields of Pearce *et al.* (1984), they are plotted in the volcanic arc and syn--collision granitoid fields (Fig. 12b). The same result is reached by plotting K_2O, Fe_2O_3 against SiO_2 and Fe_2O_3 against MgO on major-element based geotectonic classification of Maniar and Piccoli (1989), in which Artoli granitoids are plotted in the fields occupied by island arc (IAG)+continental arc (CAG)+ continental collision (CCG) granitoid (Fig. 13b-d).

DISCUSSION AND CONCLUSIONS

The major element chemistry and mineralogical compositions indicate predominance of least evolved (56.44-69.75% SiO_2) granodiorite, quartz-diorite/diorite group and limited abundance of evolved granite (69-72% SiO_2) group (Table 1, Fig. 4). According to their field relations, mineralogical and chemical compositions, the granitoids display calc-alkali affinities and metaluminous character (Fig. 7 and 8), which is confirmed by alumina saturation index (<1.1) and the < 0.78 agpaitic index (AI) (calculated as molar (Na + K)/Al).

The paleotectonic environment in which the Artoli granitoids` igneous protolith were emplaced is deduced on the Y vs. Nb diagram of Pearce *et al.* (1984), as combined volcanic arc and syn-collisional granites (Fig. 12b) and as volcanic arc granite on the (Y+Nb) vs. Rb diagram (Fig. 12a). This volcanic arc tectonic setting is supported by plotting of the samples in the pre-syn-plate collision field on the R1-R2 diagram of Batchelor and Bowden (1985), (Fig. 11), except for few data points lying in the post plate-collision field. Moreover, the low Nb contents (<11 ppm) is a characteristic of the granitoids formed in arc setting above subduction zones (Pearce, 1983). Also, when they are plotted on A/CNK vs. A/NK and SiO_2 vs. K_2O, Al_2O_3, Fe_3O_2 diagrams of Maniar and Piccoli (1989) (Fig. 13) they fall in the island arc, continental arc and continental collision granitoids fields. This is supported by the low incompatible element content particularly Nb, Ta, Y and Yb suggesting subduction/collision-related evolutionary processes.

The geochemical signature of the Artoli granitoids has all characteristics consistent with their being I-type granitoids: (1) The abundant granodiorite to quartz-diorite rocks commonly with dioritic xenoliths and rich in hornblende and biotite as mafic silicates and magnetite and titanite as accessory phases. (2) The broad compositional range, particularly in SiO_2, content (63.4-72.06 wt%). (3) The relatively high Na_2O contents

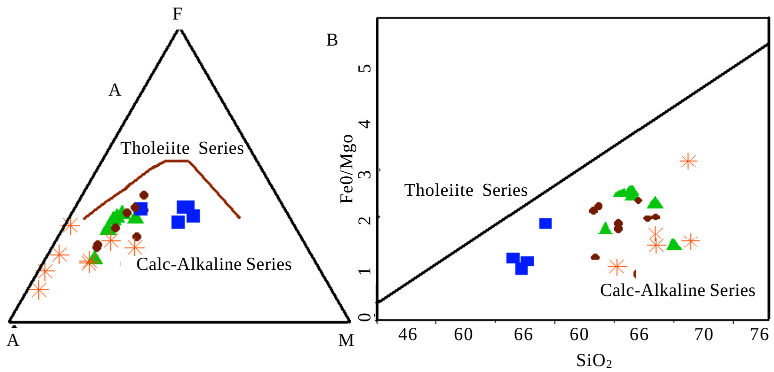

Fig. 7: (A) AFM diagram (Irvine and Baragar, 1971) and (B) SiO_2 - FeO/MgO diagram (Miyashiro, 1974) discriminating the Artoli granitoids as calc-alkaline igneous series (Symbols: as in Fig. 3)

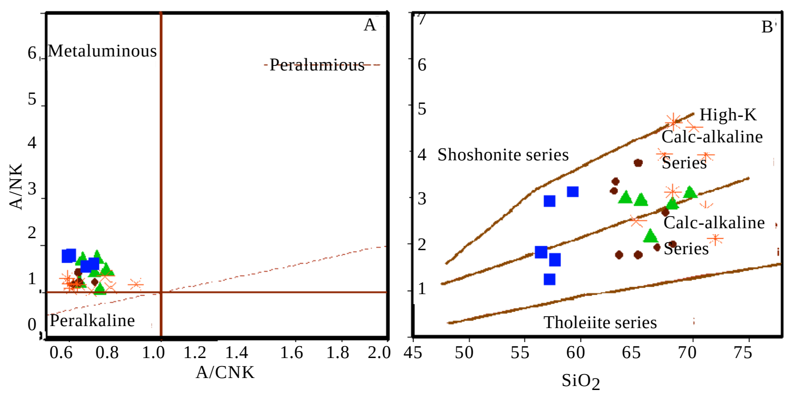

Fig. 8: (A) A/CNK = $Al_2O_3/(CaO+Na_2O+K_2O)$ vs. A/NK = $Al_2O_3/(Na_2O+K_2O$ mol.%) diagrams of Shand (1927), discriminating metaluminous, peraluminous and peralkaline compositions and (B) SiO_2-K_2O of (Peccerlio and Taylor, 1976) (Symbols: as in Fig. 3)

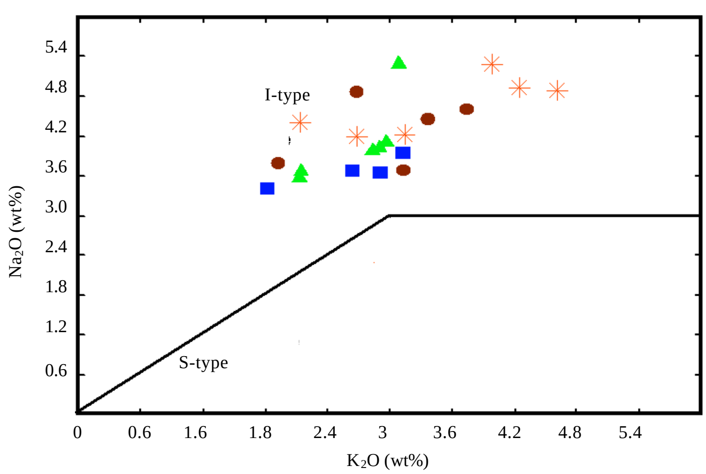

Fig. 9: Alkali concentrations discrimination diagram (K_2O - Na_2O in wt%) defining the I-type nature of the granitoids of the Artoli area (Symbols: as in Fig. 3)

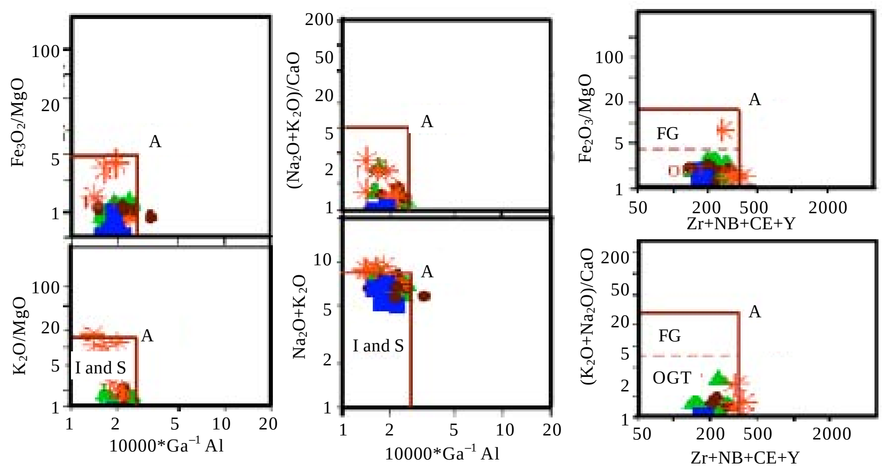

Fig. 10: Set of binary plots {Zr+Nb+Ce+Y vs Fe_2O_3/MgO and (K_2O+Na_2O)/CaO; 10000Ga/Al vs. K_2O+Na_2O, (K_2O+Na_2O)/CaO, K_2O/MgO and Fe_2O_3/MgO} proposed by (Whalen *et al*., 1987) to distinguish A-type granitoids from I- and S-types. (Major elements in in wt% and trace and REE in ppm) (Symbols: as in Fig. 3)

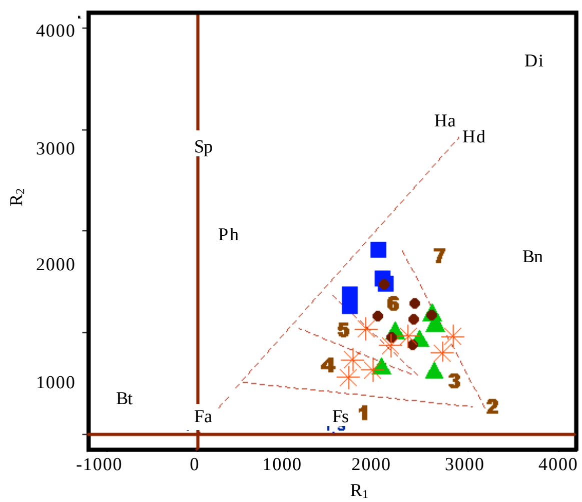

Fig. 11: R1 vs. R2 diagram of (Batchelor and Bowden, 1985) to delineate the tectonic setting of the Artoli granitoids. R1= (4Si - 11(Na + K) - 2(Fe + Ti); R_2= (6Ca + 2Mg) + Al. Fields: 1= Anorogenic 2 = Post-orogenic 3 = Syn-collision 4 = Late-orogenic 5 = Post- collision 6 = Pre-Plate collision 7 = Mantle Fractionates. (Symbols: as in Fig. 3)

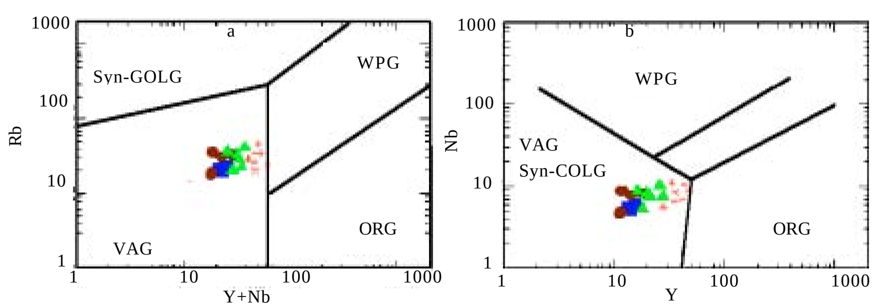

Fig. 12: (a) (Y+ Nb) vs. Rb and (b) Y vs. Nb (in ppm) discrimination digram, (Pearce *et al*., 1984), for deciphering the tectonic setting of the Artoli granitoids. ORG = Ocean ridge granites, Syn-COLG = Syn- Collisional granites, VAG = Volcanic arc granites, WPG = Within plate granites (Symbols: as in Fig. 3)

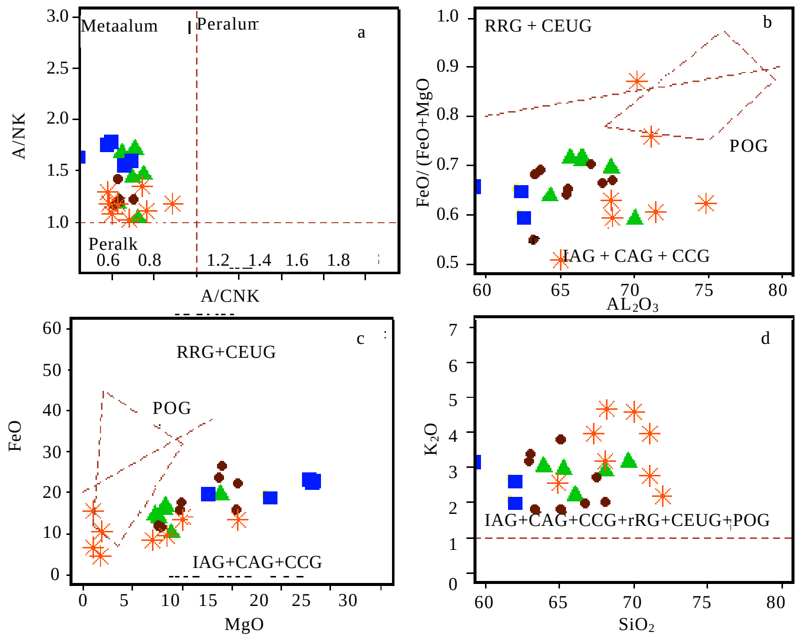

Fig. 13: Major-element based geotectonic classification of Artoli granitoids; (a) A/CNK vs. A/NK and (b-d) Binary plots SiO_2 vs. K_2O, Al_2O_3, FeO; (Maniar and Piccoli, 1989). Fields: IAG = Island Arc Granitoids, CAG = Continental Arc Granitoids, CCG = Continental Collision Granitoids, POG = Post-orogenic Granitoids, RRG = Rift-related Granitoids, CEUG = Continental Epeirogenic Uplift Granitoids, OP = Oceanic Plagiogranites. (Symbols: as in Fig. 3)

(mostly greater than 3.2%), moderate concentration of Rb,, Ba, REE and relative low Rb/Sr ratios (White and Chappell, 1983). (iv) The calc-alkaline affinity and metaluminous character (alumina saturation index, ASI less than 1.1), with generally medium-high K compositions.

The linear trends exhibited by the harker variation diagrams (Fig. 3), indicate that the granitoids are genetically related. The Artoli granitoids include rocks more felsic than diorites, MgO concentrations ccommonly >2 wt% and show negative anomaly of Ti, Nb and Hf relative to MORB indicating that the source is similar to the composition of melt produced by partial melting of the mafic lower crust (Wyllie *et al.*, 1997). On the other hand, there are rocks having relatively moderate MgO CaO, Cr and Ni contents and low SiO_2 together with LILE enrichment and low content of Th and HFSE indicating a depleted mantle origin. Thus, these results point to involvement of mantle and crust components in the generation of their protoliths.

Depending on the above account derived from integrating the field, petrographical and mineralogical investigations substantiated with the lithochemical interpretation of whole-rock analysis data, it is reasonable to conclude that:

- The area is build up of predominantly NW to N trending, Proterozoic low-grade schistosed rocks and narrow belts of high-grade metasediments into which voluminous granitoidal batholiths have been emplaced
- Chemical and mineralogical classification of the granitoids of the area, pointed out to the prevalence of intermediate and felsic rocks dominated by granodioritic to quartz dioritic/dioritic compositions, which are distinguished mineralogically by abundant hornblende and biotite with less feldspar. Throughout the region, a leucocratic biotite-hornblende granodiorite is the main rock type among these granitoids
- The lithochemical interpretation disclosed that distinctly calc-alkaline affinity, metaluminous, medium- to high-K are the characteristic features of the granitoid rocks
- The used geochemical discrimination diagrams indicate that the granitoids of the Artoli area are exclusively of I-type nature, supported by their molar values of ASI (<1.11) and the mineralogical composition, i.e., predominance of biotite and hornblende as mafic silicates and the abundance of titanite and magnetite as accessory phases

- The constructed discrimination and spider diagrams complied with the geochemical characteristics of calc-alkaline affinity, metaluminous composition, the I-type nature and the low level of Nb content suggest magmatic environment above subduction zones of volcanic arc and syn-collisional granitoids
- The petrological and geochemical data point to generation of these granitoids by partial melting in which involved mantle and mafic lower crust components
- The disclosed overall geological and geochemical characteristics of the Artoli plutonic rocks are comparable to those of the Red Sea Hills of the Nubian Shield in features pertain to calc alkaline, metaluminous affinities and I-type lithologies derived from a depleted mantle source with little or no contributions from a preexisting continental crust. The findings are in support of our previous conclusion that considers the area as a part of the westernmost Nubian Shield (Lissan and Bakhiet, 2010)

ACKNOWLEDGEMENTS

The work was partially supported by Dongola University. We would like to acknowledge the Department of Geology and Mining, University of Juba, for logistical support during the fieldwork, the Geological Research Authority of Sudan (GRAS) for the facilities offered in carrying out petrographic investigation and XRF analyses and the Rida Mining Company, Sudan who covered most of the cost of whole-rock geochemical analyses from Acme Labs. The authors wish to acknowledge with great thanks Prof. Dr. He Sheng of China University of Geosciences (Wuhan) for his valuable discussion, comments and constructive remarks on the manuscript. The authors sincerely thank Adli A/ Majeed, Madani Rajab, Dr. A/ haman Ahmed and Dr. Mutasim Adam for their contribution during field mapping.

REFERENCES

Abdelsalam, M.G., J.P. Liegeois and R.J. Stern, 2002. The saharan metacraton. J. Afr. Earth Sci., 34: 119-136.

Abdelsalam, M.G., R. Stern, J. Schandelmeier and H.M. Sultan, 1995. Deformational history of the Keraf zone in northeast sudan, revealed by shuttle imaging radar. J. Geol., 103: 475-491.

Almond, D.C., 1982. New ideas on the geological history of the Basement Complex of NE Sudan. Sudan Note Rec., 59: 106-136.

Barker, F., 1979. Trondhjemite Definition, Environment and Hypotheses of Origin. In: Trondhjemites, Dacites and Related Rocks, Barker, F. (Ed.). Elsevier, New York, pp: 1-12.

Batchelor, R.A. and P. Bowden, 1985. Petrogenetic interpretation of granitoid rock series using multicationic parameters. Chem. Geol., 48: 43-55.

Boynton, W.V., 1984. Geochemistry of Rare Earth Elements: Meteoritic Studies. In: Rare Earth Element Geochemistry, Henderson, P. (Ed.). Elsevier, Amsterdam, pp: 63-114.

Chappell, B.W. and A.J.R. White, 1974. Two contrasting granite types. Paciffic Geol., 8: 173-174.

Condie, K.C., 1998. Plate Tectonics and Crustal Evolution. Butterworth-Heinmann, London, pp: 69.

Dalziel, I.D., 1997. Overview: Neoproterozoic-paleozoic geography and tectonics: Review, hypothesis, environmental speculation. Geol. Soc. Am. Bull., 109: 16-42.

Gass, I.G., 1981. Pan-African (Upper Proterozoic) Plate Tectonics of the Arabian-Nubian Shield. In: Precambrian Plate Tectonics, Kroner, A. (Ed.). Elsevier, Amsterdam, pp: 387-405.

Grenne, T., R.B. Pedersen, T. Bjerkgard, A. Braathen, M.G. Selassie and T. Worku, 2003. Neoproterozoic evolution of Western Ethiopia: Igneous geochemistry, isotopic systematics and U-Pb ages. Geol. Mag., 140: 373-395.

Harker, A., 1909. The Natural History of Igneous Rocks. Macmillan, New York.

Irvine, T.N. and W.R.A. Barager, 1971. A guide to the chemical classification of the common volcanic rocks. Can. J. Earth Sci., 8: 523-548.

Ishikawa, Y., T. Sawaguchi, S. Iwaya and M. Horiuchi, 1976. Delineation of prospecting targets for Kuroko deposits based on modes of volcanism of underlying dacite and alteration haloes. Mining Geol., 26: 105-117.

Kroner, A., R. Greiling, T. Reischmann, I.M. Hussein, R.J. Stern, S. Durr and M. Zimmer, 1987. Pan-African crustal evolution in the segment in the Northern Africa. Am. Geophys. Union Geodyn. Ser., 17: 235-257.

Kuster, D. and J.P. Liegeois, 2001. Sr, Nd isotopes and geochemistry of the Bayuda Desert high-grade metamorphic basement (Sudan): An early Pan-African oceanic convergent margin, not the edge of the East Saharan ghost craton. Prec. Res., 109: 1-23.

Lissan, N.H. and A.K. Bakiet, 2010. The geology and geochemistry of metavolcanic rocks of artoli area, berber province, northern Sudan: An implication for petrogenetic and tectonic setting. J. Am. Sci., 6: 1-13.

Maniar, P.D. and P.M. Piccoli, 1989. Tectonic discrimination of granitoids. Geol. Soc. Mer. Bull., 101: 635-643.

Miyashiro, A., 1974. Volcanic rock series in island arcs and active continental margins. Am. J. Sci., 274: 321-355.

Neary, C.R., I.G. Gass and B.J. Cavanagh, 1976. Granitic association of Northeastern Sudan. Geol. Soc. Am. Bull., 87: 1501-1512.

Nockolds, S.R., 1954. Average chemical compositions of some Igneous rocks. Bull. Geol. Soc. Am., 65: 1007-1032.

Noweir, A.M., A.M. Abu El-Ela and B.M. Sewifi, 1990. New contributions to the geology, geochemistry and tectonic setting of the Aswan granites, southern Egypt. Qatar. Univ. Sci. Bull., 10: 395-419.

Pearce, J.A. and J.R. Cann, 1973. Tectonic setting of basic volcanic rocks determined using trace element analyses. Earth Planetary Sci. Lett., 19: 290-300.

Pearce, J.A., 1983. The Role of Sub-Continental Lithosphere in Magma Genesis at Destructive Plate Margins. In: Andesites, Orogenic Andesites and Related Rocks, Thorpe, R.S. (Ed.). Wiley and Sons, Chichester, pp: 525-548.

Pearce, J.A., N.B.W. Harris and A.G. Tindle, 1984. Trace element discrimination diagrams for the tectonic interpretation of granitic rocks. J. Petrol., 25: 956-983.

Peccerillo, A. and S.R. Taylor 1976. Geochemistry of eocene calc-alkaline volcanic rocks from the Kastamonu area, Northern Turkey. Contribut. Mineral. Petrol., 58: 63-81.

Shand, S.J., 1927. Eruptive Rocks: Their Genesis, Composition, Classification and Their Relation to Ore-deposits. Murby, London, pp: 360.

Stern, R., J., A. Kroner, R. Bender, T. Reischmann and A.S. Dawoud, 1994. Precambrian basement around Wadi Halfa, Sudan: A new perspective on the evolution of the Eastern Saharan Craton. Geol. Rundsch., 83: 564-577.

Stern, R.J. and A. Kroner, 1993. Geochronologic and isotopic constraints on Late Precambrian crustal evolution in NE Sudan. J. Geol., 101: 555-574.

Stern, R.J., 1994. Arc assembly and continental collision in the Neoproterozoic East African Orogen: Implications for the consolidation of Gondwanaland. Ann. Rev. Earth Planet. Sci., 22: 319-351.

Sun, S.S. and W.F. McDonough, 1989. Chemical and isotopic systematics of oceanic basalts: Implications for mantle composition and processes. Geol. Soc. London, 42: 313-345.

Vail, J.R., 1985. Pan-African (Late Precambrian) tectonic terrains and the reconstruction of the Arabian-Nubian Shield. Geology, 13: 839-842.

Whalen, J.B., K.L. Currie and B.W. Chappell, 1987. A-type granites: Geochemical characteristics, discrimination and petrogenesis. Contrib. Mineral. Petrol., 95: 407-419.

White, A.J.R. and L.W. Chappell, 1983. Granitoid types and their distribution in the Lachlan fold belt, Southeast Australia. Geol. Soc. Am. Memoir, 159: 21-34.

Wilson, M., 1989. Igneous Petrogenesis a Global Tectonic Approach. Chapman and Hall, London, pp: 466.

Wyllie, P.J., M.B. Wolf and S.R. van der Laan, 1997. Conditions for Formation of Tonalites and Trondhjemites: Magmatic Sources and Products. In: Greenstone Belts, De Wit, M.J. and L.D. Ashwal (Eds.). Clarendon Press, Oxford, UK., pp: 256-266.